ANTIOXIDANTS & REDOX SIGNALING
Volume 7, Numbers 1 & 2, 2005

Forum Original Research Communication

Free Radical Oxidation of Plasmalogen Glycerophosphocholine Containing Esterified Docosahexaenoic Acid: Structure Determination by Mass Spectrometry

KARIN A. ZEMSKI BERRY and ROBERT C. MURPHY

ABSTRACT

Plasmalogen phospholipids have a vinyl ether substituent at the *sn*-1 position that is susceptible to oxidative reactions that occur at cell membranes. However, the mechanism by which this oxidation occurs and the effect of the polyunsaturated fatty acid at the *sn*-2 position have not been established. To gain insight into these mechanisms, the oxidized phospholipid products resulting from the exposure of 1-*O*-hexadec-1′-enyl-2-docosahexaenoyl-*sn*-glycero-3-phosphocholine (16:0p/22:6-GPCho) to the free radical initiator 2, 2′-azobis (2-amidinopropane) hydrochloride were examined. Electrospray ionization tandem mass spectrometry, UV spectroscopy, and electron ionization–gas chromatography/mass spectrometry were used to structurally characterize the oxidized glycerophosphocholine (GPCho) products. The radical-induced peroxidation of 16:0p/22:6-GPCho revealed two major classes of oxidized phospholipids. The first class of products was formed by oxidation at the *sn*-1 position and included 1-lyso-2-docosahexaenoyl-GPCho and 1-formyl-2-docosahexaenoyl-GPCho. Additionally, the second class of oxidized products where oxidation occurred at the *sn*-2 position was classified into three categories that included chain-shortened ω-aldehydes, terminal γ-hydroxy-α,β-unsaturated aldehydes, and the addition of one or two oxygen atoms onto the *sn*-2 position of 16:0p/22:6-GPCho. These results clearly indicate that free radical-induced oxidation of plasmalogen phospholipids with esterified docosahexaenoic acid at the *sn*-2 position underwent oxidation at both the *sn*-1 and *sn*-2 positions. *Antioxid. Redox Signal.* 7, 157–169.

INTRODUCTION

PLASMALOGENS are a unique class of choline and ethanolamine glycerophospholipids that have a vinyl ether moiety rather than an ester group at the *sn*-1 position of the glycerol backbone. Plasmalogen lipids commonly have polyunsaturated fatty acyl groups such as docosahexaenoyl or arachidonoyl esterified at the *sn*-2 position of the glycerol backbone. In human cells, the percentage of plasmalogen lipids is typically ~18% of the total phospholipid mass (22); however, plasmenyl lipids can reach 50% of the total phospholipids in some cellular membranes, such as the heart, brain, red blood cells, and inflammatory cells (17). Even though the percentage of plasmalogens in certain cells is quite high, the role of these lipids in cellular membranes is not fully understood (17, 22).

The oxidation of phospholipids in biological membranes has been implicated in a variety of human diseases, such as atherosclerosis (2), ischemia (30), carcinogenesis (1), and Alzheimer's disease (19). As the hydrogen atoms on the carbon atom adjacent to the vinyl ether substituent have relatively low bond dissociation energy, plasmalogens have been suggested as targets of free radical chemistry (21), and these lipid peroxidation products have been used to assess of the severity of each of the above disease states. Previously, a protective role by plasmalogens in lipid peroxidation of cell membranes has been suggested (32). These studies showed that cells deficient in plasmalogen biosynthesis were signifi-

Cell Biology Division, Department of Pediatrics, National Jewish Medical and Research Center, and Department of Pharmacology, University of Colorado Health Sciences Center, Denver, CO.

cantly more susceptible to free radical attack compared with those cells that contained plasmalogens. From this study, it was suggested that cell membranes were protected from oxidative stress by the vinyl ether linkage of plasmalogens. Therefore, many subsequent studies have focused on the importance of the vinyl ether substituent in the antioxidant effects of plasmalogens (11, 25, 33).

Even though polyunsaturated fatty acids accumulate in plasmalogen lipids, a small number of publications have reported the chemistry that occurs at the *sn*-2 position during lipid peroxidation. It is possible that the presence of a polyunsaturated fatty acid at the *sn*-2 position plays a role in the enhanced susceptibility of plasmalogen phospholipids toward lipid peroxidation. When mixed micelles of 1-*O*-hexadec-1′-enyl-2-arachidonoyl-*sn*-glycero-3-phosphocholine (16:0p/20:4-GPCho) (GPCho) and liver-glycerophosphocholine (GPCho) were treated with Cu(II)/H_2O_2, the most abundant products were oxidized at carbon-5 of the esterified arachidonate from the plasmalogen species (14). In another study, 16:0p/20:4-GPCho was reacted with the free radical initiator 2,2′-azobis(2-amidinopropane) hydrochloride (AAPH), and various oxidation products that involved the bisallylic hydrogen position nearest to the ester moiety of the *sn*-2 position were formed (13). These studies revealed that the esterified arachidonate at the *sn*-2 position participated in oxidative reactions and could contribute to the antioxidant properties of plasmalogen lipids.

Plasmalogens constitute a major portion of the phospholipids present in the adult human brain, and a large amount of these lipids have docosahexaenoic acid esterified at the *sn*-2 position. Docosahexaenoic acid (22:6) is an *n*-3 polyunsaturated fatty acid that has five bisallylic positions and is quite vulnerable to oxidative stress (31). It has been determined that lower levels of lipid peroxides exist in brain tissue after docosahexaenoic acid supplementation (10), even though docosahexaenoic acid is highly unsaturated. One possible explanation of this behavior is that docosahexaenoic acid plays a neuroprotective role when it is at the *sn*-2 position of a plasmalogen (31). Currently, there are no studies on the role of docosahexaenoic acid in the mechanisms responsible for the protective effect of plasmalogens in terms of cellular toxicity induced by reactive oxygen species.

To gain insight into the oxidative decomposition of plasmalogen GPCho with docosahexaenoate in the *sn*-2 position, the oxidized phospholipid products resulting from the exposure of 1-*O*-hexadec-1′-enyl-2-docosahexaenoyl-*sn*-glycero-3-phosphocholine (16:0p/22:6-GPCho) to the free radical initiator AAPH were examined. Electrospray ionization tandem mass spectrometry, UV spectroscopy, and electron ionization (EI)-gas chromatography/mass spectrometry (GC/MS) were used to structurally characterize the oxidized GPCho products.

EXPERIMENTAL PROCEDURES

Materials

16:0p/22:6-GPCho and 1,2-dinonadecanoyl-*sn*-glycero-3-phosphocholine (19:0a/19:0-GPCho) were purchased from Avanti Polar Lipids, Inc. (Alabaster, AL, U.S.A.). AAPH was a gift from Dr. Joseph McCord (UCHSC, Denver, CO, U.S.A.). Methoxyamine hydrochloride (MOX), bis(trimethylsilyl)trifluoroacetamide (BSTFA), *N*-acetylcysteine (NAC), and 5% Rh/Al_2O_3 were purchased from Sigma Chemical (St. Louis, MO, U.S.A.). Sodium borohydride ($NaBH_4$) was purchased from Aldrich (Milwaukee, WI, U.S.A.). Sodium hydroxide (1 *M*) was purchased from J.T. Baker (Phillipsburg, NJ, U.S.A.). Acetyl chloride was purchased from Alltech (Deerfield, IL, U.S.A.). HPLC solvents were purchased from Fisher Scientific (Fair Lawn, NJ, U.S.A.) and used for HPLC, extraction, and hydrolysis.

Preparation of liposomes and oxidation procedure

Docosahexanoate plasmenyl glycerophosphocholine (1 μmol) in chloroform was taken to dryness under a stream of nitrogen. Large, multilamellar vesicles were formed by suspending the lipid film in 50 m*M* phosphate-buffered saline (PBS; pH 7.4) to a final concentration of 2 m*M* and vortexing the suspension for an hour at room temperature. Sonication of the large, multilamellar vesicles for 20 min resulted in the production of small, unilamellar vesicles (15). AAPH dissolved in 50 m*M* PBS (pH 7.4) was added to the phospholipid suspension for a final concentration of 10 m*M*. The reaction was carried out at 37°C for 2.5 h and was terminated by immersion in an ice bath and the addition of chloroform/methanol according to the method of Bligh and Dyer (3). The phospholipids were extracted twice with chloroform, and the organic layer was taken to dryness under a stream of nitrogen and resuspended in reversed phase solvent A (500 μl; see below). Aliquots of this sample were taken for mass spectrometric analysis.

Reversed phase chromatography (RP-HPLC) and electrospray ionization tandem mass spectrometry

Online RP-HPLC/MS/MS analysis of the chloroform layer from the oxidized plasmalogen was performed using a Chromolith Performance RP-18e (4.6 × 100 mm) column (Merck KGaA, Darmstadt, Germany). The HPLC was operated at a flow rate of 1 ml/min with a mobile phase of methanol/acetonitrile/water (60:20:20, by volume) with 1 m*M* ammonium acetate (solvent A) and 1 m*M* methanolic ammonium acetate (solvent B). The gradient was 0% solvent B to 100% solvent B in 50 min, followed by isocratic elution at 100% solvent B for 10 min. A postcolumn split was used to yield 50 μl/min into the mass spectrometer and 950 μl/min to a fraction collector, which collected two fractions per minute.

A Sciex API III$^+$ triple quadrupole mass spectrometer (PE Sciex, Toronto, Canada) was used in the positive ion mode with the orifice set at +65 V, using collision-induced dissociation (CID) to obtain a precursor ion scan of the phosphocholine ion (*m/z* 184), which is characteristic of GPCho species (23). All of the collected fractions that contained GPCho species were infused (10 μl/min) into the mass spectrometer in order to identify the oxidation products by CID in the negative ion mode. A high orifice potential was used (−98 V) in the negative ion mode in order to obtain $[M - 15]^-$ ions from the decomposition of $[M + OAc]^-$ ions. CID was performed using a collision energy of 20 V and a collision gas (argon) thickness of 190×10^{13} molecules/cm^2.

Lipid derivatization

The functional groups of certain oxidized phospholipid fractions were derivatized with BSTFA and/or MOX. Fractions of interest were derivatized by MOX using a gas-phase procedure (8). In brief, sodium hydroxide (1 ml) and MOX (83 mg) were added together and attached to an enclosed glass apparatus. During a 30-min incubation, the liberated CH_3ONH_2 gas derivatized the ketone or aldehyde groups present on the oxidized phospholipids. After MOX derivatization, BSTFA derivatives of certain oxidized phospholipid fractions were produced as previously described (28).

Michael addition reactions

NAC at 15 m*M* (64 µl) in 50 m*M* PBS (pH 7.4) and acetonitrile (256 µl) were added to certain fractions and incubated at 37°C for 4 h. The Michael addition products were introduced onto a preconditioned C_{18} solid-phase extraction tube (Supelco, Bellefonte, PA, U.S.A.) and eluted with methanol.

Saponification of phospholipids and RP-HPLC of resulting fatty acids

Oxidized phospholipid fractions of interest were hydrolyzed by the addition of acetone (125 µl) and 0.25 *M* sodium hydroxide (20 µl) for 1 h at room temperature. Dilute acetic acid (0.5%, 1 ml) was added to acidify the reaction mixture, and the fatty acids were extracted twice with 1 ml of hexane/ethyl acetate (1:1, vol/vol).

Online RP-HPLC/MS analysis of the hexane/ethyl acetate layer from the saponified lipids was performed using a Columbus 5µ C_{18} (2.0 × 150 mm) column (Phenomenex, Torrance, CA, U.S.A.). The HPLC was operated at a flow rate of 200 µl/min with a mobile phase of 8.3 m*M* acetic acid at pH 5.7 (solvent A) and 65:35 acetonitrile/methanol (solvent B). The gradient was 40% solvent B to 100% solvent B in 40 min. A postcolumn split was used to yield 20 µl/min into the mass spectrometer and 180 µl/min into photodiode array UV detector and fraction collector, which collected two fractions per minute. The Sciex API III$^+$ triple quadrupole mass spectrometer was used in the negative ion mode with the orifice at −60 V to obtain a full scan spectrum of the fatty acids present in the hexane/ethyl acetate extract.

GC/MS

Specific fractions from the above RP-HPLC separation that contained species with $[M - H]^-$ at *m/z* 343 were derivatized for structural analysis by EI-GC/MS. Catalytic reduction over 5% Rh/Al_2O_3 was performed as previously described (28). Methyl esters of the hydrogenated fatty acids were prepared by incubation with 75 µl of 3 *M* methanolic HCl (160 µl of acetyl chloride in 1 ml of methanol) at room temperature for 1 h, after which BSTFA derivatives were made as previously described (20). A gas chromatograph/mass spectrometer (Trace 2000, Thermo Finnigan, San Jose, CA, U.S.A.) was used for the EI analysis of the hydrogenated, derivatized fatty acids. The EI spectra were obtained at an electron energy of 70 eV and provided structural information regarding the hydroxyl group position from fragmentations that occur adjacent to the trimethylsilyl (TMS) ether positions (29). The same procedure was followed to prepare species with $[M - H]^-$ at *m/z* 341 from the negative ion scan for EI-GC/MS analysis, except that these compounds were first reduced with $NaBH_4$ as previously described (6).

RESULTS

The oxidation of 16:0p/22:6-GPCho and 1-palmitoyl-2-docosahexaenoyl-*sn*-glycero-3-phosphocholine (16:0a/22:6-GPCho) in the presence of AAPH was carried out for 5, 15, 30, 60, 90, 120, 180, 270, and 360 min at 37°C. RP-HPLC separation and monitoring of the starting material and the internal standard, 19:0a/19:0-GPCho, using a precursors of *m/z* 184 scan showed that the disappearance of 16:0a/22:6-GPCho was only significant after 2 h, whereas the percentage of remaining 16:0p/22:6-GPCho had already decreased by 75% (Fig. 1). This was consistent with plasmalogen GPCho lipids being more susceptible to oxidation compared with 1,2-diacyl GPCho lipids.

The products of the oxidation of 16:0p/22:6-GPCho by AAPH for 2.5 h were separated by RP-HPLC and analyzed by tandem mass spectrometry. Mass spectrometry in the positive ion mode was used to detect the oxidation products by monitoring the precursors of *m/z* 184 (Fig. 2), corresponding to the phosphocholine ion that is observed for all GPCho species (18). The starting material (16:0p/22:6-GPCho), which eluted from the reversed phase column at 45.70 min with a $[M + H]^+$ of *m/z* 790, was the major component in Fig. 2. The oxidized GPCho products of free radical oxidation were less lipophilic than the starting material and eluted from the reversed phase column between 6 and 44 min. CID in the negative ion mode with a high orifice voltage to obtain $[M - 15]^-$ ions was used to characterize the fatty acyl groups esterified to these oxidized CPCho products (23). Further structural verification was attained from the negative ion CID spectra of the intact oxidized phospholipids after the derivatization of functional groups on the fatty acyl chains with BSTFA and/or MOX.

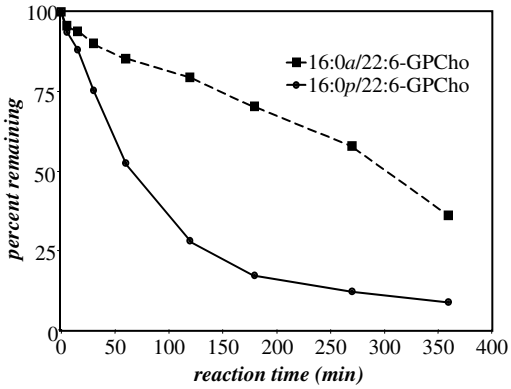

FIG. 1. Time course of the disappearance of a diacyl (16:0a/22:6-GPCho) and a plasmalogen (16:0p/22:6-GPCho) GPCho incubated in the presence of AAPH.

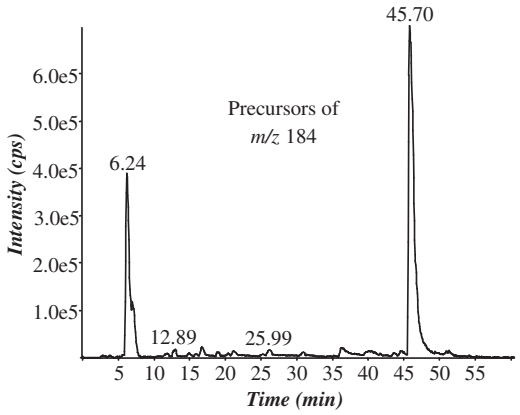

FIG. 2. RP-HPLC separation and tandem mass spectrometry analysis (LC/MS/MS) of GPCho lipids obtained after oxidation of 16:0p/22:6-GPCho with 10 m*M* AAPH. The elution of oxidized products from the RP-HPLC column was monitored by precursor ion scans of *m/z* 184, which is the GPCho-specific cation.

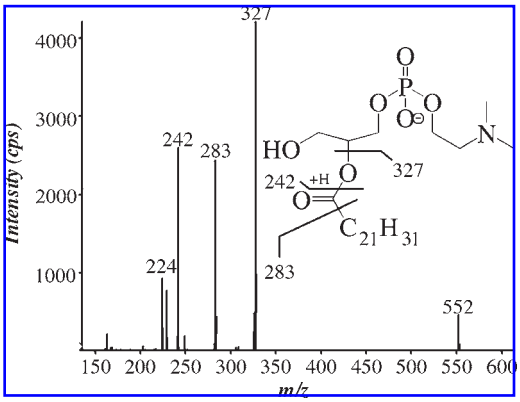

FIG. 3. CID of the [M – 15]⁻ ion derived from the oxidized GPCho product eluting from the RP-HPLC at 6.24 min. This product was identified as 1-lyso-2-docosahexaenoyl-GPCho. The origins of the ions that resulted from collisional activation are indicated in the structure of this product.

When phospholipids are oxidized by free radical events, oxidation reactions can occur at either the *sn*-1 or *sn*-2 position or both. The negative ion CID spectra were used to discern whether oxidation had occurred at the *sn*-1 or *sn*-2 position. The presence of a product ion at *m/z* 464, which corresponded to loss of the *sn*-2 substituent as a neutral ketene, in the CID spectrum of the [M − 15]⁻ of an oxidized phospholipid strongly supported that the plasmenyl chain had not been oxidized. Therefore, this product ion in the negative ion CID spectrum permitted the products observed after the oxidation of 16:0p/22:6-GPCho by AAPH to be classified by oxidation at either the *sn*-1 or *sn*-2 position.

Oxidation at the sn-*1 position*

The most abundant oxidation product eluted from the reversed phase column at 6.24 min (Fig. 2) with a $[M + H]^+$ of *m/z* 568. CID of the corresponding $[M - 15]^-$ at *m/z* 552 was consistent with the loss of the entire *sn*-1 entity during the oxidation process (Fig. 3). The CID spectrum of *m/z* 552 had an abundant ion at *m/z* 327, which corresponded to the intact carboxylate ion of docosahexaenoic acid. The product ions at *m/z* 283 and *m/z* 229 have been observed during CID of docosahexaenoic acid (12) and correspond to loss of CO_2 from the docosahexaenoate ion and fragmentation of the docosahexaenoate ion at carbon 5. The product ion at *m/z* 242 was consistent with the loss of the *sn-2* docosahexaenoyl moiety as a neutral ketene, and the *m/z* 224 product ion is loss of water from this ion. The product ions in the CID spectrum were consistent with the major oxidized phospholipid being 1-lyso-2-docosahexaenoyl-*sn*-glycero-3-phosphocholine.

The product that eluted at 7.05 min generated a $[M + H]^+$ of *m/z* 596 in the precursors of *m/z* 184 scan (Fig. 2). The CID spectrum of $[M - 15]^-$ at *m/z* 580 (Fig. 4) yielded abundant ions at *m/z* 327 and *m/z* 283, which corresponded to the docosahexaenoic acid carboxylate ion and loss of CO_2 from *m/z* 327, respectively. The other major product ion was present in the CID spectrum at *m/z* 270 and corresponded to the loss of docosahexaenoate in the *sn*-2 position as a neutral ketene species, consistent with the identification of this oxidized phospholipid as 1-formyl-2-docosahexaenoyl-*sn*-glycero-3-phosphocholine. Similar mass spectrometric behavior was observed for 1-formyl-2-arachidonoyl-*sn*-glycero-3-phosphocholine (13).

Oxidation at the sn-*2 position*

GPCho species containing ω*-aldehydes in the* sn-*2 position.* The product that eluted from the reversed phase column at 12.89 min generated a $[M + H]^+$ of *m/z* 564 (Fig. 5A), and CID of the corresponding $[M - 15]^-$ ion at *m/z* 548 produced two major product ions at *m/z* 464 and 101 (Fig. 5B). It was thought that the product ion at *m/z* 101 was a 4-oxo-butanoate carboxylate anion formed by collisional activation of the intact phospholipid. To verify this identification, the reversed phase fractions that contained a [M + H]+ at *m/z* 564

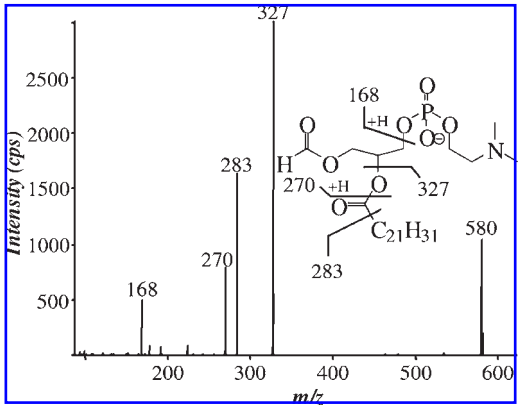

FIG. 4. CID of the [M – 15]⁻ ion derived from the oxidized GPCho product eluting from the RP-HPLC at 7.05 min. This product was identified as 1-formyl-2-docosahexaenoyl-GPCho. The origins of the ions that resulted from collisional activation are indicated in the structure of this product.

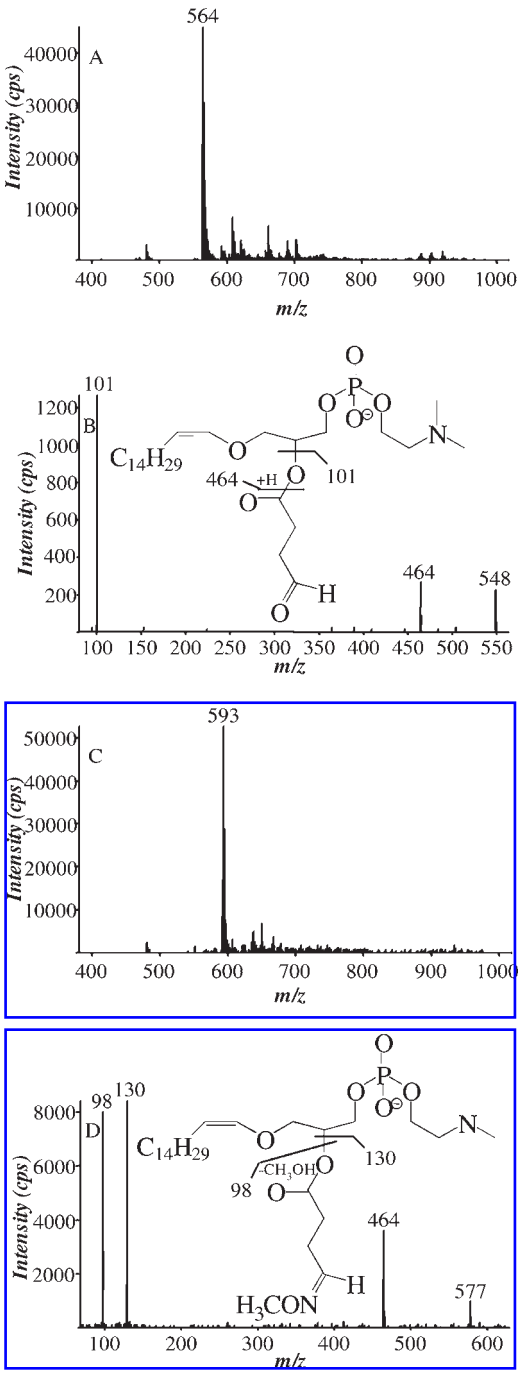

FIG. 5. (**A**) Precursors of *m/z* 184 scan of reversed phase fraction 26. The major component present in this spectrum has a $[M + H]^+$ at *m/z* 564. (**B**) CID of the $[M - 15]^-$ ion derived from the oxidized GPCho product eluting from the RP-HPLC at 12.89 min. This product was identified as 16:0p/4:0al-GPCho. The origins of the ions that resulted from collisional activation are indicated in the structure of this product. (**C**) Precursors of *m/z* 184 scan of reversed phase fraction 26 after MOX derivatization. The major component present in this spectrum has increased by 29 amu and has a [M + H]+ at *m/z* 593. (**D**) CID of the $[M - 15]^-$ ion derived from the oxidized GPCho product eluting from the RP-HPLC at 12.89 min after MOX derivatization. Note the addition of 29 amu onto the *sn*-2 position.

were derivatized with gaseous MOX. Exposure of $[M + H]^+$ at *m/z* 564 to MOX resulted in an observed mass shift to *m/z* 593, consistent with the addition of 29 amu and conversion of the terminal aldehyde to a methoxime (Fig. 5C). CID of the corresponding negative ion at *m/z* 577 (the $[M - 15]^-$ of the MOX derivative) yielded product ions at *m/z* 130 and 98 (Fig. 5D). The *m/z* 130 product ion corresponded to the 4-MOX-butanoate carboxylate anion, and *m/z* 98 was consistent with the loss of neutral methanol (32 amu) from 4-MOX-butanoate. These data were consistent with identification of this product as 1-*O*-hexadec-1′-enyl-2-[4-oxo]butanoyl-GPCho (16:0p/4:0al-GPCho). Other oxidized GPCho products similar to 16:0p/4:0al-GPCho were present in Fig. 2, and a summary of these ω-aldehyde-GPCho products is shown in Table 1. The product ions in the CID spectra of $[M - 15]^-$ of the ω-aldehyde-GPCho products before and after MOX derivatization (Table 1) were consistent with the results obtained for 16:0p/4:0al-GPCho. Therefore, it was concluded that these other compounds in Table 1 were also ω-aldehyde-GPCho products.

GPCho species containing hydroxyalkenals in the sn-*2 position.* The product that eluted from the reversed phase column at 11.82 min generated a $[M + H]^+$ observed at *m/z* 620 (Fig. 6A). The CID spectrum of the corresponding $[M - 15]^-$ ion at *m/z* 604 produced four major product ions at *m/z* 464, 157, 139, and 95 (Fig. 6B). The product ion at *m/z* 157 corresponded to the carboxylate anion from the *sn*-2 position. The additional product ions at *m/z* 139 and 95 corresponded to loss of water from the *sn*-2 carboxylate anion and loss of CO_2 from the dehydrated *sn*-2 carboxylate anion. The fragmentation pattern observed in Fig. 6B was similar to a previously published CID spectrum of the $[M - 15]^-$ of 1-palmitoyl-2-(5-hydroxy-8-oxo-oct-6-enoyl)-*sn*-glycero-3-phosphocholine, which had a terminal γ-hydroxy-α,β-unsaturated aldehyde at the *sn*-2 position, that was derived from oxidized 1-palmitoyl-2-arachidonyl-*sn*-glycero-3-phosphocholine (26). In this previously published mass spectrum, the ion *m/z* 171 was the carboxylate anion of the *sn*-2 position, and the *m/z* 153 and 109 corresponded to loss of water from the *sn*-2 carboxylate anion and loss of CO_2 from the dehydrated *sn*-2 carboxylate anion (26). To determine if $[M + H]^+$ at *m/z* 620 had a terminal γ-hydroxy-α,β-unsaturated aldehyde at the *sn*-2 position, the corresponding fractions were derivatized with MOX and BSTFA, which resulted in the disappearance of *m/z* 620 and the appearance of the abundant $[M + H]^+$ at *m/z* 721, corresponding to the addition of 101 amu (Fig. 6C). Collisional activation of the MOX/BSTFA derivative of the corresponding $[M - 15]^-$ at *m/z* 705 yielded product ions at *m/z* 258, 168, and 136 (Fig. 6D). The product ion at *m/z* 258 was consistent with the addition of 101 amu onto *m/z* 157 from the *sn*-2 radyl group. The ions at *m/z* 168 and 136 resulted from loss of trimethylsilanol (90 amu) from *m/z* 258 and loss of methanol (32 amu) from *m/z* 168. The mass spectral data before and after MOX/BSTFA derivatization supported the presence of a terminal γ-hydroxy-α,β-unsaturated aldehyde at the *sn*-2 position, and the oxidized phospholipid observed $[M + H]^+$ at *m/z* 620 was identified as 16:0p/4-hydroxy-7-oxo-hept-5-enoyl-GPCho. Other oxidized GPCho products similar to 16:0p/4-hydroxy-7-oxo-hept-5-enoyl-GPCho were present in Fig. 2, and a sum-

TABLE 1. IDENTITY OF OXIDIZED PHOSPHOLIPID PRODUCTS WITH TERMINAL ALDEHYDES IN THE *sn*-2 POSITION

GPCho compound	*Reversed phase retention time (min)*	*$[M + H]^+$*	*$[M – 15]^-$ CID products (before MOX treatment)*	*$[M – 15]^-$ CID products (after MOX treatment)*
16:0p/4:0al-GPCho	12.89	564	464	464
			101	130
				98
16:0p/6:1al-GPCho	13.13	590	464	464
			127	156
			83	112
16:0p/8:2al-GPCho	15.87	616	464	464
			159	182
			109	138
				106
16:0p/9:2al-GPCho	16.69	630	464	464
			167	196
			123	152
				120
16:0p/11:3al-GPCho	20.38	656	464	464
			193	222
			149	178
				146
16:0p/12:3al-GPCho	21.08	670	464	464
			207	236
			163	192
				160
16:0p/14:4al-GPCho	25.28	696	464	464
			233	262
			189	230
				186
16:0p/15:4al-GPCho	25.99	710	464	464
			247	276
			203	232
				200
16:0p/18:5al-GPCho	30.55	750	464	464
			287	316
			243	272
				240

Oxidized phospholipid products with terminal aldehydes in the *sn*-2 position were identified by reversed phase chromatographic retention times, *m/z* of $[M + H]^+$, $[M – 15]^-$ CID fragment ions, and $[M – 15]^-$ CID fragment ions after MOX derivatization.

mary of these hydroxyalkenal-GPCho products is shown in Table 2. The product ions in the $[M - 15]^-$ CID spectra of the other hydroxyalkenal-GPCho products before and after MOX/BSTFA derivatization (Table 2) were consistent with the results obtained for 16:0p/4-hydroxy-7-oxo-hept-5-enoyl-GPCho. Therefore, it was concluded that these other compounds in Table 2 were also hydroxyalkenal-GPCho products.

Previously, it was shown that hydroxyalkenal-GPCho could form Michael addition products with NAC (9). To verify further the presence of a terminal γ-hydroxy-α,β-unsaturated aldehyde at the *sn*-2 position, the fractions containing hydroxyalkenal-GPCho were incubated with NAC (163 g/mol) to form Michael adducts. All of the hydroxyalkenal-GPCho products that are listed in Table 2 showed similar behavior and produced Michael addition products when incubated with NAC with results similar to those discussed below. After incubation with NAC, a precursor ion scan of *m/z* 184 revealed that the $[M + H]^+$ at *m/z* 620 had diminished and that a new $[M + H]^+$ of *m/z* 783 was observed that was 163 amu higher (Fig. 7A). As there was a carboxyl group on NAC, the electrospray-generated negative ions were extracted at a decreased orifice potential (−60 V) to obtain abundant $[M - H]^-$. The CID spectrum of this $[M - H]^-$ at *m/z* 781 yielded product ions at *m/z* 464, 162, 157, 139, and 95 (Fig. 7B). The product ion at *m/z* 162 was identified as the NAC carboxylate anion, and the remaining product ions at *m/z* 157, 139, and 95 were those observed in Fig. 6B. The CID spectrum in Fig. 7B was analogous to the CID spectrum of the $[M - H]^-$ of the Michael addition product of NAC with 1-palmitoyl-2-(5-hydroxy-8-oxo-oct-6-enoyl)-*sn*-glycero-3-phosphocholine (9). Therefore, the formation of Michael adducts upon incubation of NAC with the hydroxyalkenal-GPCho products further supported the presence of a terminal γ-hydroxy-α,β-unsaturated aldehyde at the *sn*-2 position of these oxidized phospholipid products.

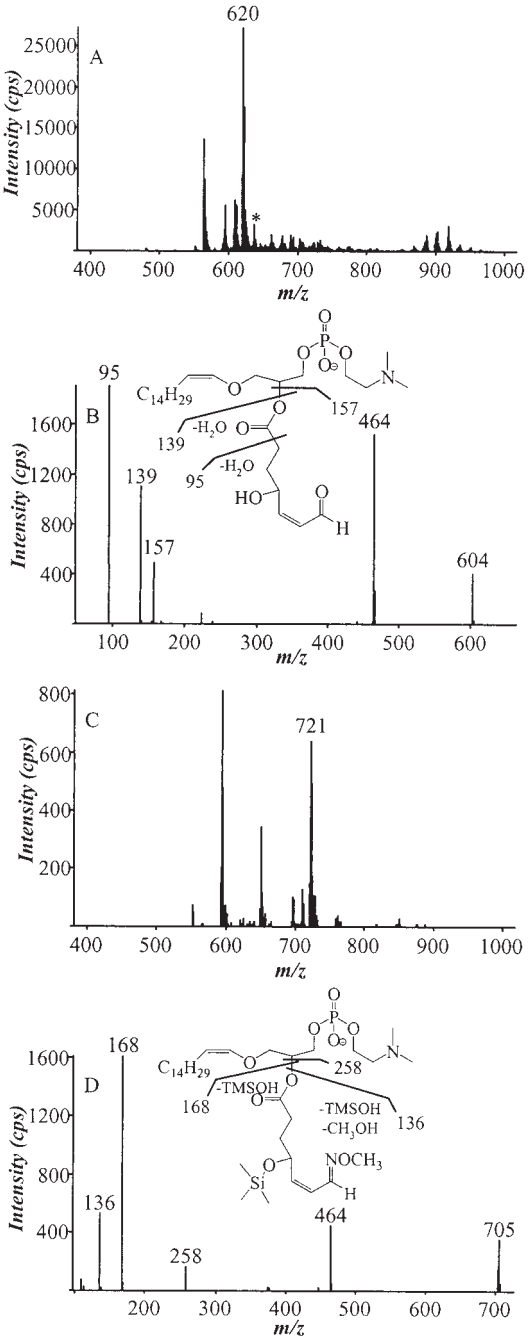

FIG. 6. **(A)** Precursors of *m/z* 184 scan of reversed phase fraction 24. The major component present in this spectrum has a $[M + H]^+$ at *m/z* 620. (**B**) CID of the $[M - 15]^-$ ion derived from the oxidized GPCho product eluting from the RP-HPLC at 11.82 min. This product was identified as 1-*O*-hexadec-1′-enyl-2-(4-hydroxy-7-oxohept-5-enoyl)-GPCho. The origins of the ions that resulted from collisional activation are indicated in the structure of this product. (**C**) Precursors of *m/z* 184 scan of reversed phase fraction 24 after MOX/BSTFA derivatization. The $[M + H]^+$ at *m/z* 620 has disappeared and increased by 101 amu to a $[M + H]^+$ at *m/z* 721. (**D**) CID of the $[M - 15]^-$ ion derived from the oxidized GPCho product eluting from the RP-HPLC at 11.82 min after MOX/BSTFA derivatization. Note the addition of 101 amu onto the *sn*-2 position.

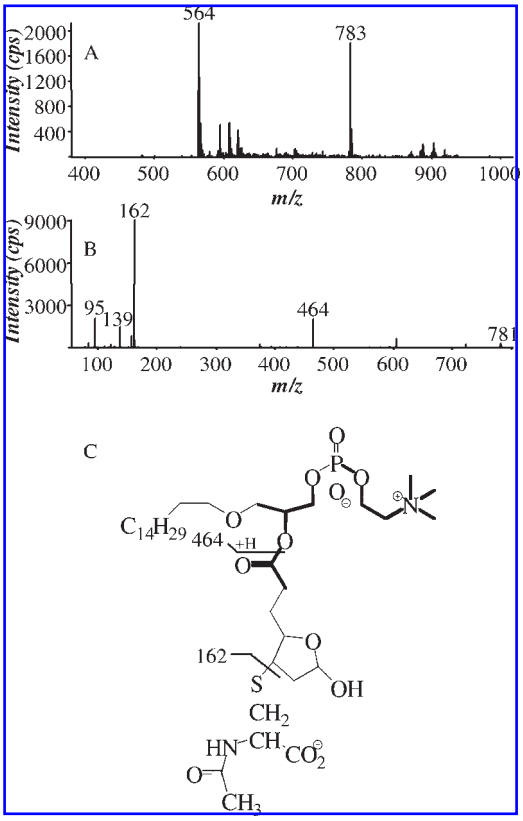

FIG. 7. (**A**) Precursors of *m/z* 184 scan of reversed phase fraction 24 after incubation with NAC. The intensity of the $[M + H]^+$ at *m/z* 620 has decreased and a $[M + H]^+$ at *m/z* 783 (addition of NAC) has appeared. (**B**) CID of the $[M - 15]^-$ ion derived from 1-*O*-hexadec-1′-enyl-2-(4-hydroxy-7-oxohept-5-enoyl)-GPCho after incubation with NAC to form Michael addition products. (**C**) The origins of the ions that resulted from collisional activation are indicated in the hemiacetal structure of the Michael adduct.

GPCho species containing one or two additional oxygen atoms in the sn-2 position. The oxidized phospholipids detected as precursors of *m/z* 184 (Fig. 2) eluting between 36 and 44 min had a $[M + H]^+$ of *m/z* 806 or 822, which corresponded to the addition of one or two oxygen atoms onto the starting material. When $[M + H]^+$ of *m/z* 806 was extracted from the precursors of *m/z* 184 scan, many products were present. The CID spectrum of the $[M - 15]^-$ anion at *m/z* 790 (Fig. 8A) from the reversed phase fraction collected from 36.5 to 37 min revealed the most abundant ion at *m/z* 343, which corresponded to the intact carboxylate anion of docosahexaenoic acid containing one additional oxygen atom, and a product ion at *m/z* 464. All of the reversed phase fractions that contained a $[M + H]^+$ of *m/z* 806 were infused into the mass spectrometer to obtain negative ion CID spectra of $[M - 15]^-$ at *m/z* 790, which were similar to Fig. 8A (data not shown). These data were consistent with the $[M + H]^+$ of *m/z* 806 products eluting between 36 and 44 min having the addition of one oxygen atom on the *sn*-2 substituent.

The extraction of those precursor ions of *m/z* 184 with $[M + H]^+$ at *m/z* 822 revealed several separable species after

TABLE 2. IDENTITY OF OXIDIZED PHOSPHOLIPID PRODUCTS WITH A TERMINAL γ-HYDROXY-α,β-UNSATURATED ALDEHYDE AT THE *sn*-2 POSITION

GPCho compound	*Reversed phase retention time (min)*	*$[M + H]^+$*	*$[M - 15]^-$ CID products (before MOX/BSTFA treatment)*	*$[M - 15]^-$ CID products (after MOX/BSTFA treatment)*
16:0p/4-hydroxy-7-oxo-hept-5-enoyl-GPCho	11.82	620	464	464
			157	258
			139	168
			95	136
16:0p/7-hydroxy-10-oxo-dec-4,8-dienoyl-GPCho	14.87	660	464	464
			197	298
			179	208
			135	176
16:0p/10-hydroxy-13-oxo-tridec-4,7,11-trienoyl-GPCho	18.99	700	464	464
			237	338
			219	248
			175	236

Oxidized phospholipid products with a terminal γ-hydroxy-α,β-unsaturated aldehyde at the *sn*-2 position were identified by reversed phase chromatographic retention times, *m/z* of $[M + H]^+$, $[M - 15]^-$ CID fragment ions, and $[M - 15]^-$ CID fragment ions after MOX/BSTFA derivatization.

the oxidation of 16:0p/22:6-GPCho by AAPH. The CID spectrum of the corresponding $[M - 15]^-$ anion at *m/z* 806 from the reversed phase fraction from 36.5 to 37 min (Fig. 8B) yielded the most abundant ion at *m/z* 341, which was consistent with the presence of a keto moiety present in the 22:6 derived from dehydration of a hydroperoxydocosahexaenoyl radyl group. As previously observed, hydroperoxy fatty acid metabolites readily lose water to yield the corresponding keto acid species during collisional activation (18). The product ion at *m/z* 297 corresponded to loss of CO_2 from the oxodocosahexaenoate ion (12). The small ion at *m/z* 359 corresponded to the intact carboxylate anion of the hydroperoxydocosahexaenoate. The presence of a nonoxidized plasmenyl chain at the *sn*-1 position was supported by the ion at *m/z* 464. Finally, the ion at *m/z* 788 was consistent with the loss of water from $[M - 15]^-$ and provided further evidence to support the presence of a hydroperoxy group on the oxidized phospholipid. The other components with $[M + H]^+$ at *m/z* 822 in the precursors of *m/z* 184 scan were analyzed by CID in the negative ion mode, and the spectra obtained were very similar to that presented in Fig. 8B. These data were consistent with a family of products corresponding to the addition of two oxygen atoms at the *sn*-2 position eluting between 36 and 44 min being docosahexaenoate with regioisomeric hydroperoxy groups.

To obtain structural information about the *sn*-2 docosahexaenoate substituents with the addition of either one or two oxygen atoms, the oxidized plasmenyl-GPCho present in the fractions eluting between 36 and 44 min was saponified and structural analysis was carried out using liquid chromatography/mass spectrometry (LC/MS), UV spectroscopy, and EI-GC/MS. The fractions eluting between 36 and 39 min, 39 and 41 min, and 41 and 44 min (Fig. 2) were pooled together so that a total of three pooled samples were saponified and extracted. Online reversed phase LC/MS analysis of the hexane/ethyl acetate layer from the saponified phospholipids was performed in the negative ion mode. When the negative ion *m/z* 343 was extracted from the resultant data array, sev-

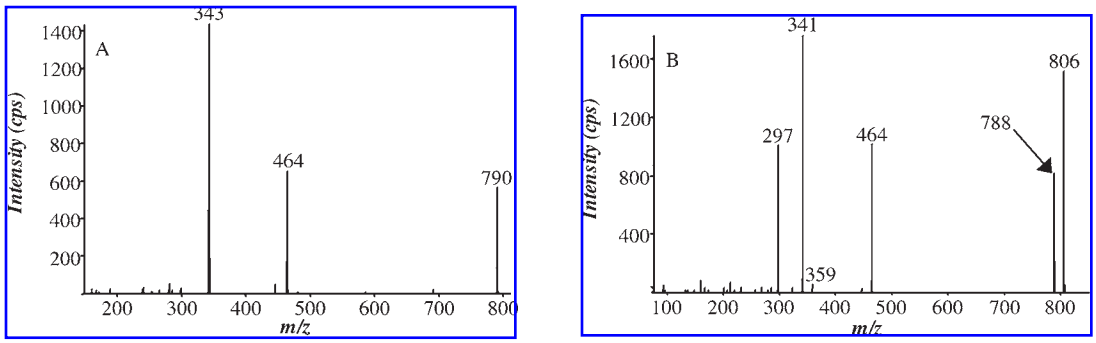

FIG. 8. (**A**) CID of the $[M - 15]^-$ ion derived from the oxidized GPCho products eluting from the RP-HPLC between 36.5 and 37 min. From this CID spectrum, it was concluded that this product contains one additional oxygen atom at the *sn*-2 position. (**B**) CID of the $[M - 15]^-$ ion derived from the oxidized GPCho products eluting from the RP-HPLC between 36.5 and 37 min. From this CID spectrum, it was concluded that this product contains two additional oxygen atoms at the *sn*-2 position.

TABLE 3. SITE OF HYDROXYLATION ON COMPOUNDS I–X

Compound	*Reversed phase retention time (min)*	*C-value*	*Major EI-GC/MS ions*	*Site of hydroxylation*
I	25.9	25	131 413	20
II	26.9	24.1	187 357	16
III	27.4	24.2	173 371	17
IV	27.9	24.0	229 315	13
V	28.4	24.0	215 329	14
VI	29.0	23.9	273 271	10
VII	30.2	24.0	287 257	11
VIII	30.5	24.0	231 313	7
IX	31.1	24.0	245 299	8
X	32.0	24.2	189 355	4

The sites of hydroxylation on compounds I–X were identified by reversed phase chromatographic retention times of *m/z* 343 and the C-values and EI-GC/MS fragment ions of the methyl ester/TMS derivatives after hydrogenation.

eral different fatty acids were detected at the reversed phase retention times shown in Table 3. Additionally, the UV absorption spectra of each HPLC components revealed a λ_{max} at 236 nm, consistent with the presence of a conjugated diene chromophore in the structure of these products. From the UV absorption spectra and positive and negative ion mass spectrometry data of the intact phospholipids, those species generating $[M - H]^-$ at *m/z* 343 were suspected to be regioisomers of hydroxydocosahexaenoic acid containing a conjugated diene. The fractions that contained *m/z* 343 were designated as compounds I–X and were catalytically reduced and derivatized as TMS/methyl esters for EI-GC/MS analysis, which was used to determine the position of the hydroxyl group (see above). A summary of these EI-GC/MS results is shown in Table 3. The major fragment ions that are listed in Table 3 were due to carbon–carbon bond cleavage adjacent to the TMS ether position (α-cleavage) (29). From these fragment ions, it was possible to identify the site of the hydroxyl group on the docosahexaenoic acid. For example, compound II had a major fragment ion at *m/z* 187 [$TMSO^+$=CH $(CH_2)_5CH_3$], suggesting a 16-hydroxylated metabolite due to α-cleavage of the C15–C16 bond. Additionally, the other major fragment ion present in the mass spectrum of compound II was *m/z* 357 [$TMSO^+$=$CH(CH_2)_{14}CO_2CH_3$], which

TABLE 4. SITE OF THE HYDROPEROXY GROUPS ON COMPOUNDS XI–XV

Compound	*Reversed phase retention time (min)*	*C-value*	*Major EI-GC/MS ions*	*Site of hydroperoxy group*
XI	26.89	25	131 413	20
XII	27.61	24.1	187 357	16
XIII	30.05	23.9	273 271	10
XIV	32.60	24.0	245 299	8
XV	33.02	24.2	189 355	4

The sites of the hydroperoxy groups on compounds XI–XV were identified by reversed phase chromatographic retention times of *m/z* 341 and the C-values and EI-GC/MS fragment ions of the methyl ester/TMS derivatives after hydrogenation and $NaBH_4$ reduction.

was also consistent with hydroxylation at carbon-16 due to α-cleavage of the C16–C17 bond. In summary, the EI spectra of hydrogenated compounds I–X defined the position of hydroxyl groups at carbons 20, 16, 17, 13, 14, 10, 11, 7, 8, and 4, respectively.

The UV spectra of all of the *m/z* 341 species (compounds XI–XV) had a λ_{max} of 236 nm that indicated the presence of a conjugated diene chromophore within the backbone of docosahexaenoic acid with a hydroperoxy group at various sites. To analyze further these hydroperoxides, each of the fractions containing *m/z* 341 was reduced with $NaBH_4$ in order to make the corresponding hydroxydocosahexaenoic acid, and the positional isomers determined by EI-GC/MS are shown in Table 4. The positional isomers of the hydroperoxydocosahexaenoic acid compounds were determined by comparing the EI-GC/MS data of the same fraction before and after $NaBH_4$ reduction. The appearance of a new hydroxydocosahexaenoic acid species after $NaBH_4$ reduction in the EI-GC/MS data indicated that the corresponding hydroperoxy compound was present in this fraction and was now detected due to $NaBH_4$ reduction. In summary, the EI spectra of hydrogenated compounds XI–XV indicated the presence of hydroperoxy groups at carbons 20, 16, 10, 8, and 4, respectively.

DISCUSSION

Plasmalogen lipids are quite susceptible to free radical oxidation (20). Early work had concentrated on the influence of the vinyl ether double bond at the *sn*-1 position, whereas the chemistry that occurred at the *sn*-2 position, where polyunsaturated fatty acids typically reside, was not examined. We have previously proposed that the polyunsaturated acids at the *sn*-2 position of plasmalogens might participate in free radical reactions because of their high abundance in these compounds and the low bond dissociation energies for the abstraction of their bisallylic hydrogen atoms. To investigate this suggestion further, the products of the free radical oxidation of 16:0p/22:6-GPCho by AAPH were identified. Various products were formed that included an *sn*-1 lysophospholipid, an *sn*-1 formyl-phospholipid, chain-shortened ω-aldehydes at the *sn*-2 position, terminal γ-hydroxy-α,β-unsaturated aldehydes at the *sn*-2 position, and the addition of one or two oxygen atoms onto the *sn*-2 position of 16:0p/22:6-GPCho.

Two of the major products that were produced upon the oxidation of 16:0p/22:6-GPCho by AAPH involved oxidation of the vinyl ether substituent at the *sn*-1 position, while retaining docosahexaenoate at the *sn*-2 position. These products were identified as 1-lyso-2-docosahexaenoyl-*sn*-glycero-3-phosphocholine (OH/22:6-GPCho) and 1-formyl-2-docosahexaenoyl-*sn*-glycero-3-phosphocholine (1:0a/22:6-GPCho). It is thought that both of these products originated from an *sn*-1 hydroperoxy hemiacetal and were formed by subsequent decomposition of this intermediate through two different pathways (13). One of the pathways would result in the formation of an alkoxy radical by homolytic cleavage of the O-O bond of the hydroperoxy group (27). Hydrogen atom abstraction by the alkoxy radical would result in a hemiacetal that could be easily hydrolyzed to generate the major reaction product, OH/22:6-GPCho. It is thought that the formation of 1:0a/22:6-GPCho also occurred through the *sn*-1 hydroperoxy hemiacetal by this intermediate undergoing a Hock rearrangement well known for allylic hydroperoxides (7), resulting in 1:0a/22:6-GPCho and pentadecanal.

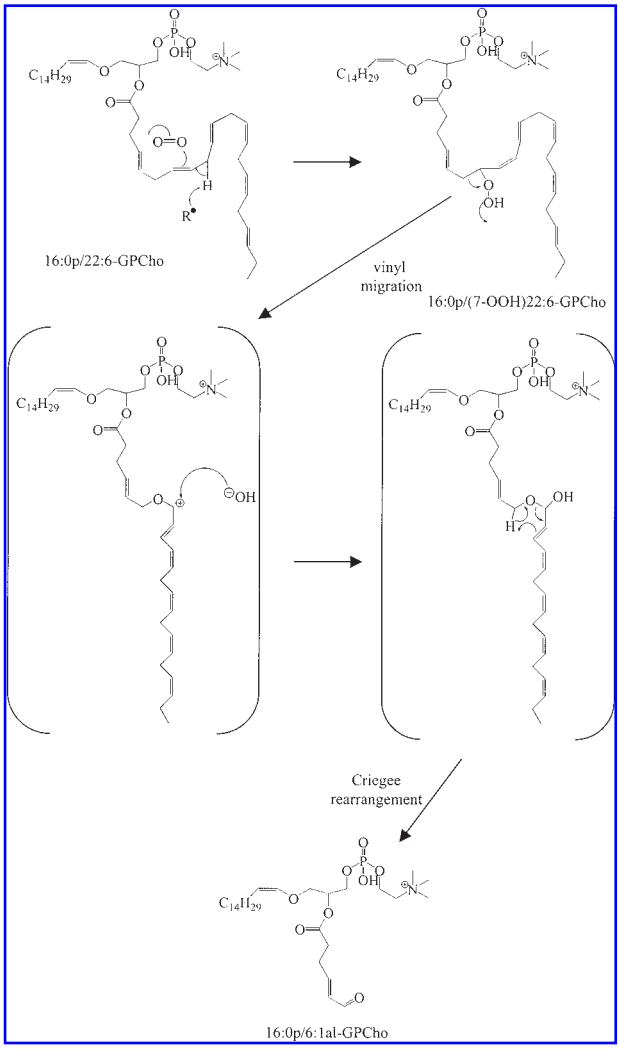

FIG. 9. The proposed mechanism for the formation of terminal aldehydes formed at the bisallylic positions of docosahexaenoic acid, specifically 16:0p/6:1al-GPCho.

Oxidation of docosahexaenoate at the *sn*-2 position, while retaining the vinyl ether in the *sn*-1 position, was also observed during the oxidation of 16:0p/22:6-GPCho with AAPH. The minor oxidized products that were formed at the *sn*-2 position could be classified into three categories that included chain-shortened ω-aldehydes, terminal γ-hydroxy-α,β-unsaturated aldehydes, and the addition of one or two oxygen atoms onto the *sn*-2 position of 16:0p/22:6-GPCho. Previous investigations considered the mechanisms of plasmalogen oxidation as only involving the vinyl ether substituent followed by decomposition of the radyl *sn*-1 group. However, it is apparent from these experiments that the oxidation of 16:0p/22:6-GPCho in cellular membranes also involved the oxidation of docosahexaenoic acid.

Two interesting classes of *sn*-2 oxidation products included the addition of one or two oxygen atoms to the docosa-

hexaenoyl group with $[M + H]^+$ at *m/z* 806 or 822 and reversed phase retention times from 36 to 44 min. Upon extracting $[M + H]^+$ at *m/z* 806 and 822 from the precursors of *m/z* 184 scan, it was found that there were 10 major compounds with $[M + H]^+$ at *m/z* 806 and five major products with $[M + H]^+$ at *m/z* 822. These products were identified after saponification of the fatty acids from the glycerol backbone by EI-GC/MS, and it was determined that hydrogen abstraction occurred at all five of the bisallylic sites of docosahexaenoic acid. The position of the hydroxy or hydroperoxy group and presence of a conjugated diene were consistent with the known mechanism of hydrogen abstraction and addition of molecular oxygen at the terminal carbon atoms of the pentadienyl radical.

These results were in slight contrast to the results that were obtained upon the oxidation of 16:0p/20:4-GPCho with AAPH (13), where the products that underwent oxidation at the *sn*-2 position involved predominant oxidation at carbon-5. However, other products of arachidonic acid oxygenation at the next two additional bisallylic carbon atoms were also observed. The proposed mechanism of radical reactions of plasmalogen phospholipids with arachidonate in the *sn*-2 position included the initial formation of a hemiacetal hydroperoxy radical that would propagate the abstraction of the first bisallylic hydrogen at carbon-7 of arachidonate (21). If this mechanism was favored in the reactions of 16:0p/22:6-GPCho with AAPH, carbon-4 oxygen-containing products would have resulted. However, these species were not the major products observed.

From the results reported herein, it is clear that free radical events proceed through the formation of hydroperoxy radicals from the docosahexaenoyl acyl group without the oxidation of the *sn*-1 vinyl ether group. It was possible that docosahexaenoate could directly participate in the free radical propagation reactions due to the positioning of a susceptible bisallylic methylene group close to the polar region of the bilayer without involvement of the *sn*-1 position. Even though the major products that were observed did not indicate an intermolecular interaction between the *sn*-1 and *sn*-2 positions, it is clear from the time course in Fig. 1 that 16:0p/22:6-GPCho disappears much faster than 16:0a/22:6-GPCho, and that the vinyl ether group in the *sn*-1 position does have an effect on the susceptibility of the phospholipid to free radical attack by formation of the major free radical product as the *sn*-1 lyso species.

Another class of *sn*-2 oxidation products that were formed upon the oxidation of 16:0p/22:6-GPCho were terminal ω-aldehydes in the *sn*-2 position. These products were identified by the $[M - 15]^-$ CID spectra of both the 16:0p/[ω-aldehyde]-GPCho product and the MOX-derivatized product (Fig. 5 and Table 1). The general mechanism of formation of 16:0p/4:0al-GPCho, 16:0p/8:2al-GPCho, 16:0p/11:3al-GPCho, and 16:0p/14:4al-GPCho most likely involved the initial formation of an allylic hydroperoxide that could then undergo migration of the vinyl substituent (Hock rearrangement) and would result in an aldehyde attached to the glycerophospholipid backbone (13).

There were additional ω-aldehyde products, which included 16:0p/6:1al-GPCho, 16:0p/9:2al-GPCho, 16:0p/12: 3al-GPCho, 16:0p/15:4al-GPCho, and 16:0p/18:5al-GPCho, that had to be formed by a mechanism different from that described

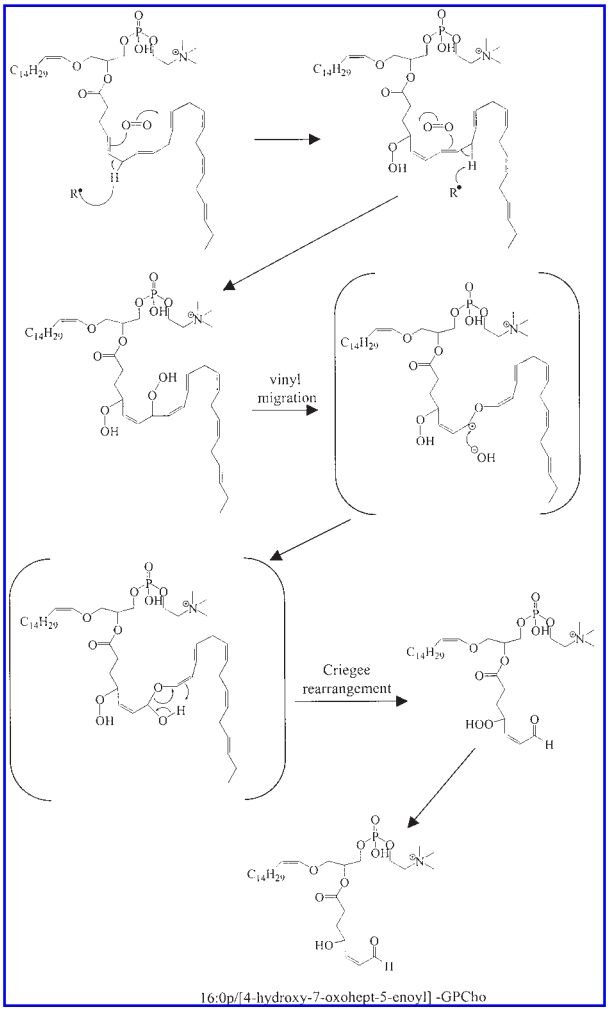

FIG. 10. The proposed mechanism for the formation of 16:0p/4-hydroxy-7-oxo-hept-5-enoyl-GPCho.

above. These particular products can be characterized as terminal aldehydes formed at the bisallylic positions of docosahexaenoic acid. A mechanism consistent with the formation of these particular ω-aldehydes, using 16:0p/6:1al-GPCho as an example, would involve the initial formation of a 7-hydroperoxy-docosahexaenoate at the *sn*-2 position (Fig. 9) typically observed upon the oxidation of unsaturated fatty acids. This intermediate has both an adjacent vinylic and allylic group. The mechanism of formation of the previously mentioned ω-aldehyde products was explained by a Hock rearrangement with vinyl group migration, but this rearrangement does not account for the formation of these other ω-aldehyde products. Therefore, it is proposed that, instead of a vinylic rearrangement, an allylic migration occurred. This allylic migration would lead to cleavage between carbon-6 and carbon-7, which would result in the formation of two aldehydes that included a 16:0p/6:1al-GPCho. Generally, an allylic migration would not be expected to predominate over a vinylic migration; however, migration of methylene groups has been reported for hydroperoxides (5).

The last group of *sn*-2 oxidation products observed had a terminal γ-hydroxy-α,β-unsaturated aldehyde at the *sn*-2 po-

sition. These products were identified by the $[M - 15]^-$ CID spectra both before and after MOX/BSTFA derivatization (Fig. 6 and Table 2). Additionally, the presence of a terminal γ-hydroxy-α,β-unsaturated aldehyde at the *sn*-2 position was confirmed when Michael addition products were observed upon incubation with NAC. These terminal γ-hydroxy-α,β-unsaturated aldehydes were similar in structure to 4-hydroxy-2E-nonenal (4-HNE), a widely studied aldehyde product of lipid peroxidation (4). The mechanism of formation of these terminal γ-hydroxy-α,β-unsaturated aldehyde compounds from unsaturated fatty acids has been a matter of debate. However, it has been proposed that 4-hydroperoxy-2E-nonenal (4-HPNE) is an immediate precursor of 4-HNE (16). Brash and co-workers formulated two distinct mechanisms of the formation of 4-HPNE from the methyl terminus of linoleic acid (24). The first mechanism was explained by a Hock rearrangement of a 10,13-dihydroperoxide formed from linoleic acid. The second mechanism of 4-HPNE production involved the formation of 9-hydroperoxyoctadecadienoic acid (9-HpODE), which underwent a Hock rearrangement and cleaved into 9-oxononanic acid and 3Z-nonenal, which was then oxygenated to 4-HPNE. In addition to forming a terminal γ-hydroxy-α,β-unsaturated aldehyde on the methyl terminus of linoleic acid, Brash and co-workers also described formation of γ-hydroxy-α,β-unsaturated aldehydes at the carboxy terminus when 9-HpODE underwent the first mechanism or when 13-HpODE underwent a rearrangement by the second mechanism (24). It is possible that the mechanism of formation of the hydroxyalkenal-GPCho products that were observed upon the oxidation of 16:0p/22:6-GPCho could be similar to one proposed by Brash and co-workers (24). Figure 10 illustrates the formation of a 4,7-dihydroperoxydocosahexanoate at the *sn*-2 position. This product has allylic hydroperoxy groups, which can undergo a Hock rearrangement and result in cleavage between carbon-7 and carbon-8 and the formation of two aldehyde fragments that includes a hydroperoxyalkenal-GPCho species (Fig. 10). This hydroperoxyalkenal-GPCho could then be reduced to the corresponding hydroxyalkenal-GPCho by homolytic cleavage of the hydroperoxy group. This proposed mechanism is supported by a component with an $[M + H]^+$ at *m/z* 620 that eluted at 11.82 min (Fig. 6A). Also, a minor component eluted with a $[M + H]^+$ at *m/z* 636, which might be a hydroperoxyalkenal-GPCho. Unfortunately, this product was formed in low abundance and could not be further characterized. It should be mentioned that the other hydroxyalkenal-GPCho products that produced a $[M + H]^+$ at *m/z* 660 or 700 also had corresponding hydroperoxyalkenal-GPCho $[M + H]^+$ at *m/z* 676 and 716.

The radical-induced peroxidation of 16:0p/22:6-GPCho has revealed several new oxidized phospholipids. The major products of oxidation, *sn*-1 lyso/22:6-GPCho and 1:0a/22:6-GPCho, were formed due to the chemical reactivity of the vinyl ether bond of the *sn*-1 position and accounted for the rapid disappearance of the majority of this plasmalogen. However, many other products were observed where oxidation of docosahexaenoyl at the *sn*-2 position occurred, suggesting that the chemical reactivity of the *sn*-1 vinyl ether and the bisallylic methylene groups of the *sn*-2 docosahexaenoate are independently susceptible to free radical reactions.

ACKNOWLEDGMENTS

This work was supported in part by a grant from the National Institutes of Health (HL34303).

ABBREVIATIONS

1:0a/22:6-CPCho, 1-formyl-2-docosahexaenoyl-*sn*-glycero-3-phosphocholine; 16:0p/4:0al-GPCho, 1-*O*-hexadec-1′-enyl-2-[4-oxo]butanoyl-*sn*-glycero-3-phosphocholine; 16:0p/20:4-GPCho, 1-*O*-hexadec-1′-enyl-2-arachidonoyl-*sn*-glycero-3-phosphocholine; 16:0a/22:6-GPCho, 1-palmitoyl-2-docosahexaenoyl-*sn*-glycero-3-phosphocholine; 16:0p/22:6-GPCho, 1-*O*-hexadec-1′-enyl-2-docosahexaenoyl-*sn*-glycero-3-phosphocholine; 19:0a/19:0-GPCho, 1,2-dinonadecanoyl-*sn*-glycero-3-phosphocholine; 22:6, docosahexaenoic acid; AAPH, 2,2′-azobis(2-amidinopropane) hydrochloride; BSTFA, bis (trimethylsilyl)trifluoroacetamide; CID, collision-induced dissociation; EI, electron ionization; GC/MS, gas chromatography/mass spectrometry; GPCho, glycerophosphocholine; 4-HNE, 4-hydroxy-2E-nonenal; 4-HPNE, 4-hydroperoxy-2E-nonenal; 9-HpODE, 9-hydroperoxyoctadecadienoic acid; LC/ MS, liquid chromatography/mass spectrometry; LC/MS/MS, liquid chromatography/tandem mass spectrometry; MOX, methoxyamine hydrochloride; $NaBH_4$, sodium borohydride; NAC, *N*-acetylcysteine; OH/22:6-GPCho, 1-lyso-2-docosahexaenoyl-*sn*-glycero-3-phosphocholine; PBS, phosphate-buffered saline; RP-HPLC, reversed phase high-performance liquid chromatography; TMS, trimethylsilyl.

REFERENCES

1. Athar M. Oxidative stress and experimental carcinogenesis. *Indian J Exp Biol* 40: 656–667, 2002.
2. Berliner JA and Heinecke JW. The role of oxidized lipoproteins in atherogenesis. *Free Radic Biol Med* 20: 707–727, 1996.
3. Bligh EG and Dyer WJ. A rapid method of total lipid extraction and purification. *Can J Biochem Physiol* 37: 911–917, 1959.
4. Esterbauer H, Schaur RJ, and Zollner H. Chemistry and biochemistry of 4-hydroxynonenal, malonaldehyde, and related aldehydes. *Free Radic Biol Med* 11: 81–128, 1991.
5. Frimer AA. The reaction of singlet oxygen with olefins: the question of mechanism. *Chem Rev* 79: 359–387, 1979.
6. Fu S, Hick LA, Sheil MM, and Dean RT. Structural identification of valine hydroperoxides and hydroxides on radical-damaged amino acid, peptide, and protein molecules. *Free Radic Biol Med* 19: 281–292, 1995.
7. Gardner HW and Plattner RD. Linoleate hydroperoxides are cleaved heterolytically into aldehydes by a Lewis acid in aprotic solvent. *Lipids* 19: 294–299, 1984.
8. Harrison KA, Davies SS, Marathe GK, McIntyre T, Prescott S, Reddy KM, Falck JR, and Murphy RC. Analy-

sis of oxidized glycerophosphocholine lipids using electrospray ionization mass spectrometry and microderivatization techniques. *J Mass Spectrom* 35: 224–236, 2000.
9. Hoff HF, O'Neil J, Wu Z, Hoppe G, and Salomon RL. Phospholipid hydroxyalkenals: biological and chemical properties of specific oxidized lipids present in atherosclerotic lesions. *Arterioscler Thromb Vasc Biol* 23: 275–282, 2003.
10. Hossain MS, Hashimoto M, Gamoh S, and Masumura S. Influence of docosahexaenoic acid on cerebral lipid peroxide level in aged rats with and without hypercholesterolemia. *Neurosci Lett* 244: 157–160, 1998.
11. Ingrand SS, Wahl A, Favreliere S, Barbot F, and Tallineau C. Quantification of long-chain aldehydes by gas chromatography coupled to mass spectrometry as a tool for simultaneous measurement of plasmalogens and their aldehydic breakdown products. *Anal Biochem* 280: 65–72, 2000.
12. Kerwin JL, Wiens AM, and Ericsson LH. Identification of fatty acids by electrospray mass spectrometry and tandem mass spectrometry. *J Mass Spectrom* 31: 184–192, 1996.
13. Khaselev N and Murphy RC. Structural characterization of oxidized phospholipid products derived from arachidonate-containing plasmenyl glycerophosphocholine. *J Lipid Res* 41: 564–572, 2000.
14. Khaselev N and Murphy RC. Peroxidation of arachidonate containing plasmenyl glycerophosphocholine: facile oxidation of esterified arachidonate at carbon-5. *Free Radic Biol Med* 29: 620–632, 2000.
15. Kumar A and Gupta CM. Transbilayer distributions of red cell membrane phospholipids in unilamellar vesicles. *Biochim Biophys Acta* 769: 419–428, 1984.
16. Lee SH and Blair IA. Characterization of 4-oxo-nonenal as a novel product of lipid peroxidation. *Chem Res Toxicol* 13: 698–702, 2000.
17. Lee TC. Biosynthesis and possible biological functions of plasmalogens. *Biochim Biophys Acta* 1394: 129–145, 1998.
18. MacMillan DK and Murphy RC. Analysis of lipid hydroperoxides and long-chain conjugated keto acids by negative ion electrospray mass spectrometry. *J Am Soc Mass Spectrom* 6: 1190–1201, 1995.
19. Montine TJ, Neely MD, Quinn JF, Beal MF, Markesbery WR, Roberts LJ II, and Morrow JD. Lipid peroxidation in aging brain and Alzheimer's disease. *Free Radic Biol Med* 33: 620–626, 2002.
20. Morand OH, Zoeller RA, and Raetz CR. Disappearance of plasmalogens from membranes of animal cells subjected to photosensitized oxidation. *J Biol Chem* 263: 11597–11606, 1988.
21. Murphy RC. Free-radical-induced oxidation of arachidonoyl plasmalogen phospholipids: antioxidant mechanism and precursor pathway for bioactive eicosanoids. *Chem Res Toxicol* 14: 463–472, 2001.
22. Nagan N and Zoeller RA. Plasmalogens: biosynthesis and functions. *Prog Lipid Res* 40: 199–229, 2001.
23. Pulfer M and Murphy RC. Electrospray mass spectrometry of phospholipids. *Mass Spectrom Rev* 22: 332–364, 2003.
24. Schneider C, Tallman KA, Porter NA, and Brash AR. Two distinct pathways of formation of 4-hydroxynonenal. *J Biol Chem* 276: 20831–20838, 2001.
25. Stadelmann-Ingrand S, Favreliere S, Fauconneau B, Mauco G, and Tallineau C. Plasmalogen degradation by oxidative stress: production and disappearance of specific fatty aldehydes and fatty alpha-hydroxyaldehydes. *Free Radic Biol Med* 15: 1263–1271, 2001.
26. Subbanagounder G, Deng Y, Borromeo C, Dooley AN, Berliner JA, and Salomon RG. Hydroxy alkenal phospholipids regulate inflammatory functions of endothelial cells. *Vascul Pharmacol* 38: 201–209, 2002.
27. Swern D (Ed). *Organic Peroxides, Volume II*. New York: Wiley–Interscience, 1971, p. 86.
28. Wheelan P, Zirrolli JA, Morelli JG, and Murphy RC. Metabolism of leukotriene B_4 by cultured human keratinocytes. *J Biol Chem* 268: 25439–25448, 1993.
29. Wheelan P, Zirrolli JA, and Murphy RC. Analysis of hydroxy fatty acids as pentafluorobenzyl ester, trimethylsilyl ether derivatives by electron ionization gas chromatography/mass spectrometry. *J Am Soc Mass Spectrom* 6: 40–51, 1995.
30. Witztum JL and Steinberg D. Role of oxidized low density lipoprotein in artherogenesis. *J Clin Invest* 88: 1785–1792, 1991.
31. Yavin E, Brand A, and Green P. Docosahexaenoic acid abundance in the brain: a biodevice to combat oxidative stress. *Nutr Neurosci* 5: 149–157, 2002.
32. Zoeller RA, Morand OH, and Raetz CRH. A possible role for plasmalogens in protecting animal cells against photosensitized killing. *J Biol Chem* 263: 11590–11596, 1988.
33. Zoeller RA, Lake AC, Nagan N, Gaposchkin DP, Legner MA, and Lieberthal W. Plasmalogens as endogenous antioxidants: somatic cell mutants reveal the importance of the vinyl ether. *Biochem J* 338: 769–776, 1999.

Address reprint requests to:
Robert C. Murphy, Ph.D.
Department of Pharmacology
Mail Stop 8303
University of Colorado HSC
P.O. Box 6511
Aurora, CO 80045-0511

E-mail: robert.murphy@uchsc.edu

Received for publication May 10, 2004; accepted August 23, 2004.

This article has been cited by:

1. Ana Reis, Corinne M. Spickett. 2012. Chemistry of phospholipid oxidation. *Biochimica et Biophysica Acta (BBA) - Biomembranes* **1818**:10, 2374-2387. [CrossRef]
2. Valerie B. O'Donnell. 2011. Mass spectrometry analysis of oxidized phosphatidylcholine and phosphatidylethanolamine. *Biochimica et Biophysica Acta (BBA) - Molecular and Cell Biology of Lipids* . [CrossRef]
3. Agnieszka Broniec, Radoslaw Klosinski, Anna Pawlak, Marta Wrona-Krol, David Thompson, Tadeusz Sarna. 2011. Interactions of plasmalogens and their diacyl analogs with singlet oxygen in selected model systems. *Free Radical Biology and Medicine* **50**:7, 892-898. [CrossRef]
4. Hock Rearrangement . [CrossRef]
5. M. Rosário M. Domingues, Cláudia Simões, João Pinto da Costa, Ana Reis, Pedro Domingues. 2009. Identification of 1-palmitoyl-2-linoleoyl-phosphatidylethanolamine modifications under oxidative stress conditions by LC-MS/MS. *Biomedical Chromatography* **23**:6, 588-601. [CrossRef]
6. I Labadaridis, M Moraitou, M Theodoraki, G Triantafyllidis, J Sarafidou, H Michelakakis. 2009. Plasmalogen levels in full-term neonates. *Acta Paediatrica* **98**:4, 640-642. [CrossRef]
7. M DOMINGUES, A REIS, P DOMINGUES. 2008. Mass spectrometry analysis of oxidized phospholipids. *Chemistry and Physics of Lipids* **156**:1-2, 1-12. [CrossRef]
8. Beate Fuchs, Karin Müller, Frank Göritz, Steffen Blottner, Jürgen Schiller. 2007. Characteristic Oxidation Products of Choline Plasmalogens are Detectable in Cattle and Roe Deer Spermatozoa by MALDI-TOF Mass Spectrometry. *Lipids* **42**:11, 991-998. [CrossRef]
9. M KOPANI, P CELEC, L DANISOVIC, P MICHALKA, C BIRO. 2006. Oxidative stress and electron spin resonance. *Clinica Chimica Acta* **364**:1-2, 61-66. [CrossRef]
10. Jason D. Morrow . 2005. Introduction for Special Forum Issue on Isoprostanes and Related Compounds. *Antioxidants & Redox Signaling* **7**:1-2, 153-156. [Citation] [Full Text PDF] [Full Text PDF with Links]